Analyst

Accepted Manuscript

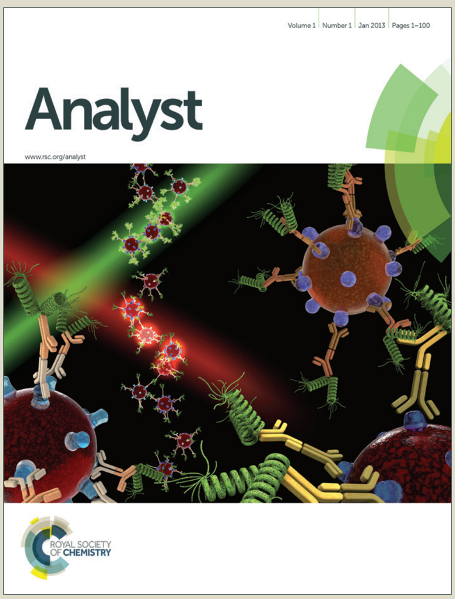

Cite this: DOI: 10.1039/c0xx00000x

www.rsc.org/xxxxxx

ARTICLE TYPE

Electrochemical Detection of pM-Levels of Urokinase Plasminogen Activator by Phosphorothioated RNA Aptamer: Improved Affinity and Suppression of Interference from Nonspecific Adsorption of BSA

Marta Jarczewska[a,b], Laszlo Kekedy-Nagy[a], Jesper S. Nielsen[a,c], Rui Campos[a], Jørgen Kjems[a,c], Elżbieta Malinowska[b], Elena E. Ferapontova[a,*]

Received (in XXX, XXX) Xth XXXXXXXXX 20XX, Accepted Xth XXXXXXXXX 20XX
DOI: 10.1039/b000000x

Protein biomarkers of cancer allow a dramatic improvement in cancer diagnostics as compared to traditional histological characterisation of tumours by enabling non-invasive analysis of cancer development and treatment. Here, an electrochemical label-free assay for urokinase plasminogen activator (uPA), a universal biomarker of several cancers, has been developed based on the recently selected uPA-specific fluorinated RNA aptamer, tethered to a gold electrode via a phosphorothioated dA tag, and soluble redox indicators. Binding properties of the uPA-aptamer couple and interference from non-specific adsorption of bovine serum albumin (BSA) were modulated by the electrode surface charge. A nM uPA electroanalysis at positively charged surfaces, complicated by the competitive adsorption of BSA, was tuned to the pM uPA analysis at negative surface charges of the electrode, being improved in the presence of negatively charged BSA. The aptamer affinity for uPA displayed via the binding/dissociation constant relationship correspondingly increased, ca. three orders of magnitude, from 0.441 to 367. Under optimal conditions, the aptasensor allowed 10^{-12} - 10^{-9} M uPA analysis, also in serum, being practically useful for clinical applications. The proposed strategy for optimization of the electrochemical protein sensing is of particular importance for assessment and optimization of *in vivo* protein ligand binding by surface-tethered aptamers.

Introduction

Timely performed cancer diagnosis is critical for successful treatment of cancer and prognosis of tumour progression and individual response to treatment.[1, 2] The routinely used histological analysis of tumors somehow restricts cancer diagnosis to either external or internal late-stage tumours that may be already too late to treat, and current efforts are focused on selection and analysis of such biomarkers of cancer that can be found in physiological fluids, such as serum/blood, saliva, and urine, and used for molecular-level characterisation of tumours.[3-5]. In this context, certain proteins dis-regulated in specific types of cancer may be considered as reliable cancer biomarkers, in particular, prostate-specific antigen (PSA) recommended by the American Cancer Society for prostate cancer screening in serum,[6, 7] breast- and ovarian cancer indicative HER-2/neu,[8, 9] human ovarian biomarker CA125,[10, 11] and lymphoma-and colorectal cancer-related CD30.[12, 13]

Recent studies showed that urokinase plasminogen activator (uPA) can be considered as a prognostic biomarker of several types of cancer.[14, 15] The urokinase activation system formed by a cascade of proteolytic enzymes and regulators is involved in degradation of extracellular matrix proteins and cellular migration during cancer invasion and metastasis.[16, 17] uPA itself is a serine protease of ca. 54 kDa[18] secreted in its inactive pro-uPA form that binds to the cell-surface uPA receptor uPAR.[14, 17] Upon binding, pro-uPA is activated to uPA that regulates the action of other proteases and is able to catalyse the cleavage of plasminogen to plasmin, leading to the extracellular proteolysis.[14, 17] Increased uPA levels are correlated with the development of ovarian cancer,[19] squamous cell carcinoma,[20] and breast cancer,[21] and thus may be used for reliable diagnosis of cancer, either by immunohistochemistry[22] or ELISA.[23, 24]

Protein assays exploiting aptamers,[25, 26] especially their inexpensive and instrumentally simple electrochemical formats,[27-30] may be considered as a challenging alternative to immunoassays. High-specificity of aptamers that can be *in vitro* selected for almost all possible ligands[31-34] transforms aptamers into exclusive biorecognition units, which binding properties and instrumental translation of the biorecognition reaction can be modulated and optimized in a variety of ways, such as the overall non-trivial design of aptamer sequences[35-37] and variation of the electrode[38, 39] and medium properties.[40] Such optimisation is particularly important in *in vivo* and *in vitro* clinical protein assays (e.g thrombin,[41-44] lysozyme,[45] platelet-derived growth factor[46, 47] and interferon[48] assays) practically complicated by low physiological concentrations of protein biomarkers and interferences from non-specific adsorption of other proteins present in physiological samples.

Recently, a series of RNA aptamers with high affinity for uPA have been selected.[49] 79 and 33 nucleotide (nts) RNA sequences exhibited affinities for uPA, estimated as a half-maximum inhibitory concentration IC_{50}, of 5 nM and 11.6 nM, correspondingly. The aptamers strongly inhibited interactions between uPA and uPAR, as well as activation of plasminogen, and thus were chosen for electrochemical analysis of uPA. To stabilize the aptamers against ribonuclease digestion and chemical cleavage, the RNA aptamer sequences were selected from the pool of RNAs with hydrogen in 2' hydroxyl group of the ribose ring substituted for fluorine (Figure 1). The fluorinated aptamers showed higher affinity for uPA as compared to the non-modified ones.[49]

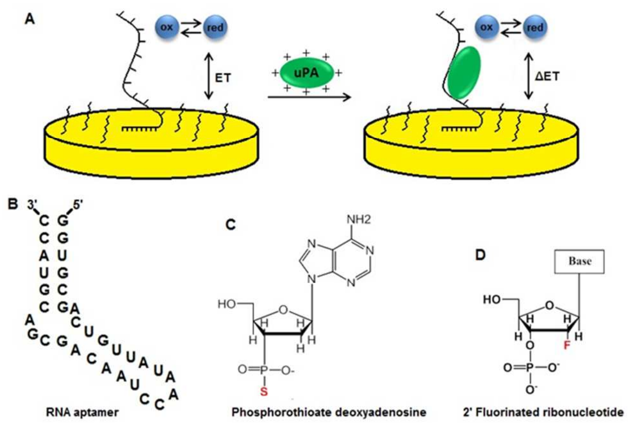

Fig. 1. (A) Schematic representation of the RNA aptasensor for uPA and structures of (B) 33 nts RNA aptamer, (C) phosphorothioate deoxyadenosine and (D) 2'-fluorinated ribonucleotide

An electrochemical assay with soluble redox indicators[50] was chosen as a cost-effective approach that does not require expensive redox labelling of the fluorinated RNA aptamer and still allows reliable and straightforward analysis of the protein-aptamer binding producing essential interfacial changes.[44, 45, 51, 52] The aptamer was tethered to the electrode surface via a phosphorothioated adenosine tag (dA*, Figure 1B), enzymatically introduced into the 3´- end of the RNA aptamer sequence (Figure 1). DNA immobilization onto gold via the dA* tag demonstrated improved stability of the DNA-gold binding as compared to the commonly used alkanethiol linkers, while, at the same time, cheapening of the production of the tag-modified fluorinated RNA aptamer sequence as compared to the automated RNA synthesis protocols.[53]

uPA binding to the surface-tethered aptamer was electrochemically interrogated at differently charged electrode surfaces corresponding to the potential windows of two redox indicators used, ferricyanide and methylene blue (MB). That allowed electrostatic and redox indicator-associated modulation of the electrode-solution interfacial properties relative binding of uPA and a competitive protein, BSA, to the surface-tethered aptamer. The aptamer affinity for its ligand protein was also improved, becoming three orders of magnitude higher compared to that shown in solution.

Experimental

Materials

Bovine serum albumin (BSA, MW 66.5 kDa, p*I* 4.7), methylene blue (MB), urea and all the components of buffer solutions were purchased from Sigma-Aldrich, Germany. Fetal bovine serum was from Invitrogen, Life Technologies, Carlsbad, USA, sodium dodecyl sulfate (SDS) was from AppliChem GmbH, Germany, human two-chain uPA (MW 48.5 kDa, p*I* 8.8) was from Wakamoto Pharmaceutical Company, Japan, 6-mercapto-1-hexanol (MC_6OH) was from Fluka, Germany, potassium ferricyanide ($K_3Fe(CN)_6$) was from Merck, Germany and SH-C_{11}-(ethylene glycol)$_3$-OH (SH-C_{11}-(EG)$_3$-OH) from ProChimia Surfaces, Poland. All solutions were prepared with Milli-Q water (18 MΩ, Millipore, Bedford, MA, USA). Control DNA sequence with a dA*$_5$ tag at 3´-end: 5'-GTT GTG CAG CGC CTC ACA AC A*A*A*A*A*-3' was synthesized by Metabion International AG, Martinsried, Germany.

The 2'-F uPA aptamer with poly-dA* phosphorothioated tag was prepared according to the following protocol. RNA aptamer was transcribed from a double stranded DNA template (TAT<u>GAATTC</u>ATTAATACGACTCACTATAGGTGCGCTGT TATAACCTAACAGCGACGTACC) using T7 Y639F. Transcription was carried for 16 h at 37 °C in 80 mM HEPES, pH 7.5, containing 20 mM $MgCl_2$, 30 mM DTT, 1 mM spermidine-HCL, 100 µg mL^{-1} BSA, 2.5 mM each ATP and GTP (Sigma Aldrich, Germany) and 2.5 mM each 2´-F-dCTP and 2´-F-dUTP (Metkinen Chemistry, Finland). RNA was subsequently gel purified and extracted using electroelution. The integrity of the RNA was verified by electrophoresis and the quality of the RNA was checked by UV absorbance measurements. For 3´-end labelling, 200 pmol of RNA was incubated with PolyA polymerase (New England Biolabs, USA) and 1 mM phosphorothioated adenosine (ATPγS) for 30 min. Successful labelling was confirmed by gel electrophoresis. Following tag labelling, the RNA was subjected to phenol/chloroform extraction followed by ethanol precipitation.

Electrode Modification

Prior to electrochemical measurements, gold electrodes (2 mm diameter, CH, Instruments, Austin, USA) were incubated in piranha solution (H_2SO_4: H_2O_2, 1:3 (v/v)) for 30 min and then washed with water. Then the electrodes were electrochemically cleaned in 0.5 M NaOH by cycling the electrode between -0.5 and -1.4 V (10 cycles, scan rate 0.05 V s^{-1}), mechanically polished on a microcloth pad in 1 µm diamond and 0.1 µm alumina slurries (Struers, Copenhagen, Denmark) followed by rinsing with water and ultrasonication in the ethanol/water solution (1:1 (v/v)) for 10 min, and finally electrochemically polished in 1 M H_2SO_4 (cycling from -0.3 to 1.7 V, 10 cycles, scan rate 0.3 V s^{-1}) and in 0.5 M H_2SO_4/10 mM KCl (cycling from 0 to 1.7 V, 10 cycles, scan rate 0.3 V s^{-1}). The electrochemical surface area of electrodes estimated by integration of the gold surface oxide reduction peak in 0.1 H_2SO_4 was 0.069 ± 0.013 cm^2. The clean electrodes were thoroughly rinsed with Mili-Q water and then kept in absolute ethanol before any modification.

The aptamer/MC_6OH-modified electrodes were prepared by placing 10 µL of 5 µM RNA aptamer solution (in 5 mM

NaH_2PO_4/Na_2HPO_4 containing 50 mM NaCl and 100 mM $MgCl_2$, pH 7) onto the electrode surface, covered with a lid and incubated at 4^0 C overnight. The aptamer-modified electrodes were then rinsed with a buffer solution and incubated in 2 mM solution of MC_6OH in 20 mM NaH_2PO_4/Na_2HPO_4, containing 0.15 M NaCl (PBS), pH 7.4, for 30 min. The aptamer/SH-C_{11}-$(EG)_3$-OH-modified electrodes were prepared by incubating aptamer-modified electrode in 2 mM SH-C_{11}-$(EG)_3$-OH in 20 mM PBS for 1 h. The MC_6OH-modified electrodes were prepared by incubation in solution of 2 mM MC_6OH in PBS, pH 7.4, for 30 min, while the SH-C_{11}-$(EG)_3$-OH - modified electrodes were prepared by incubation in solution of 2 mM SH-C_{11}-$(EG)_3$-OH in PBS, pH 7.4, for 1 h. After rinsing with PBS, the electrodes were directly used for experiments. For protein analysis, the aptamer-modified electrodes were incubated for 30 min in protein-containing either PBS, pH 7.4, or PBS containing 10% serum. After incubation, the electrodes were rinsed with PBS and used for electrochemical measurements. In processing serum data, they were referred to the signals observed after exposure of the electrodes to 10% serum/PBS in the absence of uPA.

Instrumentation

All electrochemical experiments were conducted in a conventional three-electrode cell using Autolab electrochemical systems (AUT85280, Methrom, Utrecht, Netherlands) equipped with a NOVA-1.8.17 software. A Pt wire and an Ag/AgCl (3M KCl) (Sigma-Aldrich, Germany) electrodes were utilized as auxiliary and reference electrode, respectively. Electrochemical impedance spectroscopy (EIS) measurements were recorded at 0.2 V with $K_3Fe(CN)_6$ and at -0.225 V with MB as redox indicator (frequency range from 100 kHz to 0.4 Hz). Cyclic voltammetry (CV) in presence of MB was conducted in the range from 0 to -0.5 V and scan rates from 3 to 0.05 V s^{-1} and differential pulse voltammetry (DPV) was performed in the range from 0 to -0.5 V, pulse amplitude 25 mV, step potential 5 mV, apparent scan rate 0.1 V s^{-1}. Prior experiments, working solutions were deaerated with Ar for 5 min and then kept under Ar flow during the whole experimental period, though this procedure did not affect the final results.

Results and Discussion

Electroanalysis of biological molecules can be complicated by undesirable adsorption of proteins present in physiological fluid such as blood/serum [54] containing predominantly serum albumins (2/3 of the total protein content) and globulins (1/3). [55] In a small-molecule analysis their interference may be overcome by sample filtration, [56] which is not applicable to the protein analysis, and thus alternative ways of combatting non-specific protein adsorption should be considered. Electrode surface antifouling modification [57, 58] and appropriate experimental conditions such as solution composition[59] and potential window of the assay[38, 60] may allow to diminish and even exclude interference of non-specific protein adsorption on the assay outcome.

Impedimetric analysis of uPA binding with ferricyanide as a redox indicator

Non-specific adsorption of BSA was most pronounced at a bare gold surface (ESI, Figure S1), as revealed by the routinely used assay with a soluble redox indicator ferricyanide.[50] BSA blocks the electrode surface and impedes the redox reaction of the indicator, while modification of the electrode by MC_6OH and DNA improves the antifouling properties of the surface (ESI, Figure S1). Then, a well-developed electrochemistry of the ferri/ferrocyanide couple can be followed both from CVs and EIS recorded with the MC_6OH-modfied and DNA/MC_6OH-modified electrodes after their interaction with BSA (ESI; Figures S1, S2). Interestingly, serum depressed only the electrochemical signal at bare gold electrodes, while for all other systems the redox reaction of ferricyanide in the absence and presence of serum proceeded with close efficiencies (Figure S3, S4). Quite similar data were obtained with uPA, also in the presence of BSA (ESI, Figure S5-S7). For both proteins, BSA and uPA, their non-specific adsorption on MC_6OH, SH-C_{11}-$(EG)_3$-OH, and arbitrary DNA-modified electrodes was insufficient to produce a statistically attributable change in the electrochemical signal, such as electron transfer resistance, R_{ET}, represented by the charge transfer semicircle in the impedance spectra (no pronounced increase in R_{et} that might be expected for the protein-blocked surface).

In contrast, a concentration dependent change in the R_{ET} reflecting a specific binding of uPA to the RNA aptamer sequence tethered to the gold surface via the phosphorothioated dA* tag could be followed in Figure 2A, inset, starting from 1 nM uPA. Under experimental conditions used (pH 7.4) the uPA protein is positively charged. Then, its specific binding to the aptamer should result in structural rearrangement of the aptamer ("condensation"-like) increasing the negative surface charge density and also introducing an additional electron transfer (ET) barrier, by this impeding the ET reaction of ferricyanide on the protein/RNA layer.

The EIS response of the aptamer-modified electrode (MC_6OH as a co-adsorbate) displayed a characteristic high-frequency charge transfer semicircle, reflecting the resistance of the modified electrode in the ET reaction of ferricyanide, and a low frequency Warburg region consistent with the diffusion of the indicator to the electrode surface (Figure 2A, inset). The data were fitted to the Randles circuit consisting of the solution resistance, ET resistance R_{ET}, electric double layer (EDL) capacitance and the Warburg element.[56] The R_{ET} increased with the increasing uPA concentration, and the R_{ET} variation normalized to the R_{et} value in the absence of uPA ($\Delta R_{ET} = R_{ET} - R_{ET,0}$) indeed depended on the uPA concentration (Figure 2A), indicating the uPA binding to the aptamer–modified surface.

To find the best coordinates for analysis of uPA binding to the aptamer-modified surface, the total impedance $|Z|$ and phase shift (θ) dependences on the frequency, represented by the Bode plots were constructed (Figure 2B). It can be seen that the most unambiguous signal changes occur in the low, 1 to 10 Hz frequency range, where the total impedance essentially increased with uPA concentration. For the phase shift an inversion of the signal variation occurred at 5 Hz. Impedimetric response variations at frequencies above 10 kHz were minor and not monotonic (Figure S12, ESI). Therefore, it was clear that binding of uPA to the aptamer induces the most significant signal changes at low frequencies and those data are most useful for analysis of the protein-aptamer binding.

Cite this: DOI: 10.1039/c0xx00000x

www.rsc.org/xxxxxx

ARTICLE TYPE

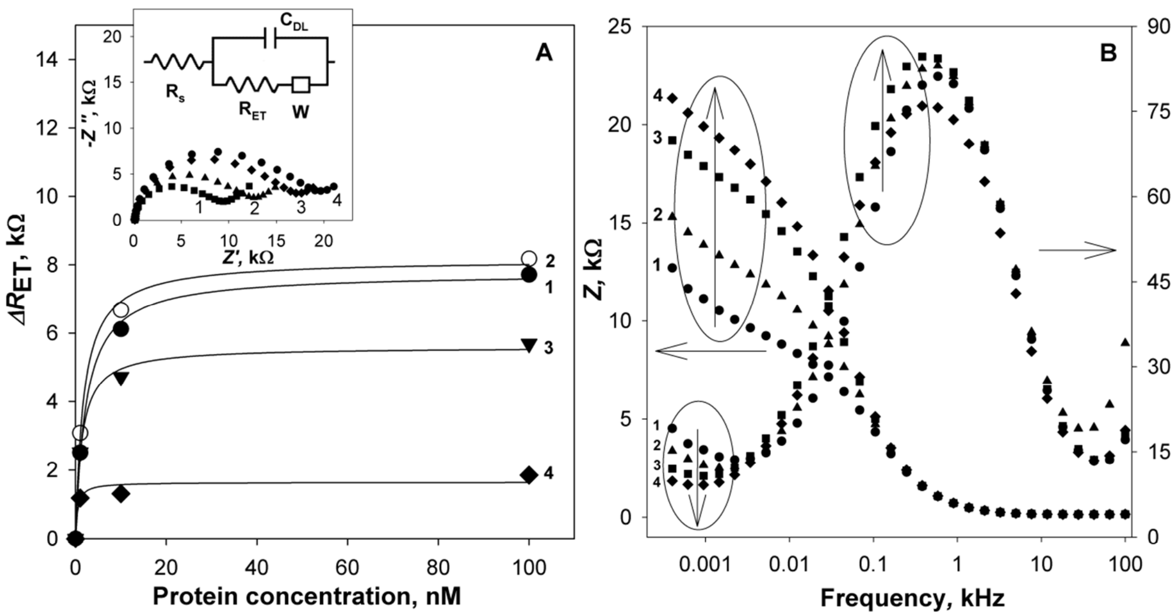

Fig. 2. (A) Variation of the ET resistance, ΔR_{ET}, with the protein concentrations constructed from the EIS data recorded with the aptamer-modified electrode for 30 min incubated in solutions of (1) uPA, (2) uPA and 100 nM BSA, (3) BSA and (4) uPA and serum. The data were fitted to the Langmuir adsorption isotherm and Scatchard's model. (Inset) Nyquist plots for the same electrodes recorded in (1) PBS and after 30 min incubation in (2) 1 (3) 10, and (4) 100 nM uPA solutions; the Randles circuit used for fitting EIS data shown. (B) Bode plots for the aptamer-electrode recorded in (1) PBS and after 30 min incubation in (2) 1, (3) 10 and (4) 100 nM uPA solutions. Measurement potential: 0.2 V, frequency range: 100 kHz - 0.4 Hz; redox indicator: 2 mM $K_3Fe(CN)_6$ in 20 mM PBS, pH 7.4.

Since the EIS signal change stemmed from the protein binding, the surface binding equilibrium and kinetics were evaluated by fitting the ΔR_{ET}–[uPA] data to the simplest adsorption and binding isotherms, such as the Langmuir adsorption isotherm:

$$S = S_{max} \times K_b \times [P]/(1 + K_b \times [P]) \quad (1)$$

and that of the Scatchard model[57]

$$S = S_{max} \times [P]/(K_d + [P]), \quad (2)$$

where S is the electrochemical signal, K_b is the constant reflecting the relation between the protein binding/dissociation constants at aptamer–modified surface, K_d is the dissociation constant, and [P] is the protein concentration. The K_b and K_d were also calculated from the $|Z|$ and θ data, and values very similar to those evaluated from the ΔR_{ET}–[uPA] dependence were obtained.

It can be seen from the fitting analysis that binding of uPA to the aptamer-modified surface yields $K_b < 1$, indicating slightly higher dissociation rate (Table 1). The dissociation constant K_d of 2.27 nM approached the values shown in solution.[49]

Table 1. Binding (K_b) and dissociation (K_d) constants obtained with the aptamer/MC_6OH-modified electrodes at positively charged (q^+, ferricyanide as a redox indicator) and negatively charged (q^-, methylene blue as a redox indicator) electrode surfaces.

	K_b (q^+) from ΔR_{ET}	K_b (q^-) from $((I-I_0)/I_0)\times100\%$	K_d (q^+) / nM from ΔR_{ET}	K_d (q^-) / nM from $((I-I_0)/I_0)\times100\%$
uPA	0.568	86.7	2.27	0.012
uPA/100 nM BSA	0.441	367.0	1.76	0.003
BSA	0.770	58.0	1.30	0.017
uPA/serum	n.a.	n.a.	n.a.	0.006

n.a.:non-applicable

Specificity of the uPA biorecognition by the surface-tethered aptamer was tested in the presence of negatively charged BSA, shown to electrostatically regulate and actually improve specificity of uPA binding to the aptamer in solution.[49] The impedimetric response in the presence of 100 nM BSA steadily increased with the increasing concentration of uPA (Figures S8, ESI and 2A, curve 2), and a minor improvement in the dissociation constant (K_d of 1.76 nM) was observed. However, considering positive charges of the electrode surface, it was suggested that BSA molecules might compete with the uPA for surface binding sites. Control experiments performed solely with

BSA indicated that BSA adsorbed onto the aptamer-modified electrode surface (Figure S9, ESI), though with the apparent efficiency lower than uPA (Figure 2A, curve 3). It is important to note, that even minor adsorption of the negatively charged BSA could lead to the pronounced changes of the EIS signal, resulting from the additional electrostatic repulsion of the negatively charge ferricyanide. Nonspecific interactions of BSA with the RNA-aptamer-modified surface were quite strong, with the K_b of 0.77 and the K_d of 1.299 nM, and BSA adsorption could not be reduced neither by the MC_6OH replacement by a longer blocking agent, SH-C_{11}-$(EG)_3$-OH, [57, 58] nor by ionic surfactants such as SDS[59] (Figures S10 and S11, ESI). Along with that, the BSA interference with the uPA assay was not additive: namely, the signal increase due to the uPA binding in the presence of BSA was much less than might be expected from the individual BSA and uPA signals (Figure 2A).

Interestingly, ferricyanide/DNA-aptamer assays for cationic thrombin [61, 62] and lysozyme [45] were shown not to be affected by BSA, though BSA is known to produce ionic complexes with DNA in solution.[63] BSA adsorption on the DNA-modified electrodes studied here was also insignificant in terms of EIS signal variation (Figure S1, ESI). That implies a quite specific structural and/or electrostatic regulation of the BSA binding to the RNA aptamer tethered to the electrode surface.

Albumins are most abundant proteins in the blood/serum,[56] and since BSA adsorption on the positively charged RNA-aptamer-modified surface was significant, even worse situation would be expected in more complex media such as serum, with serum proteins non-specifically adsorbing onto the RNA-aptamer modified surface.[54, 56] To minimize BSA adsorption, further electroanalysis was performed with a methylene blue redox probe operating within the negative potential window, where adsorption of serum proteins was shown to be insignificant and not interfering with electrochemical assays.[38, 56]

Impedimetric analysis of uPA with methylene blue as a redox indicator

MB as a redox indicator offers several advantages over ferricyanide, due to the negative potential window of its redox activity and ability to bind to both proteins and nucleic acids.[28, 50] This might allow to avoid interference from nonspecific adsorption of proteins.[51] uPA binding to the aptamer- modified electrode was impedimetrically studied in presence of MB, and ESI spectra different from those in presence of $K_3Fe(CN)_6$ where recorded (compare Figure 3A and Figure 2A, inset).

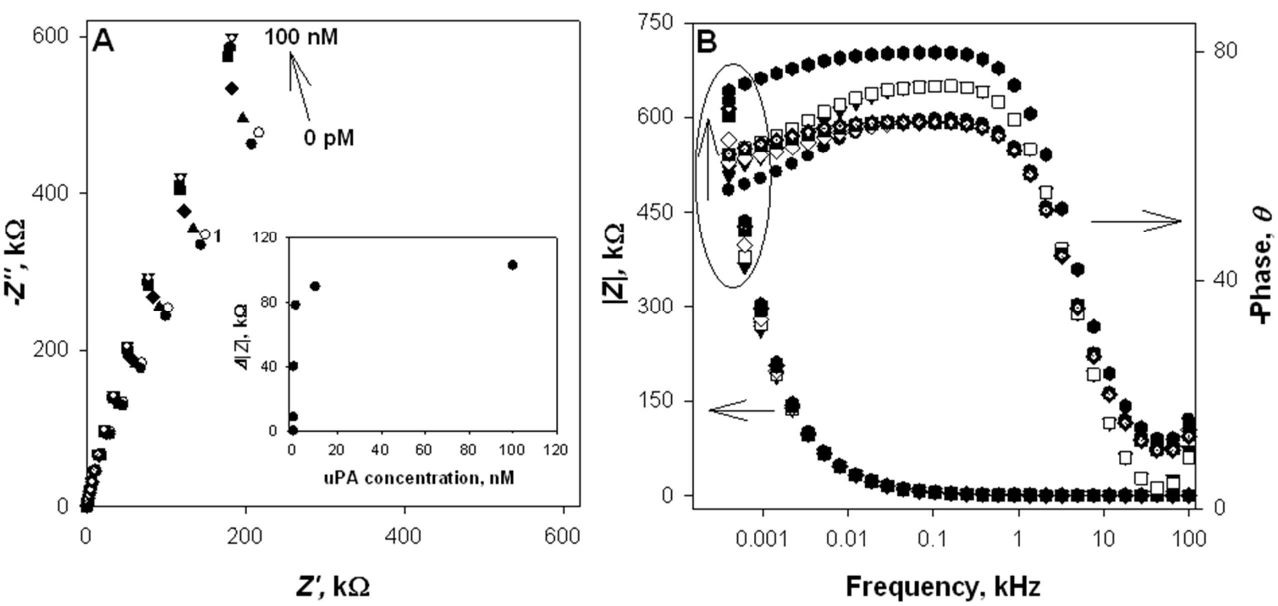

Fig. 3. The EIS spectra, presented in (A) Nyquist plot and (B) Bode plot coordinates, recorded with the aptamer-modified electrode in 1 µM MB solution in 20 mM PBS, pH 7.4, before and after 30 min incubation in 1 pM - 100 nM uPA solutions. The measurement potential was -0.225 V. (Inset) Dependence of $\Delta|Z|$ and phase shift (θ) on the uPA concentration at 0.4 Hz.

The EIS spectra recorded in MB solutions did not show the charge-transfer semicircle, earlier observed with ferricyanide as a soluble redox indicator, though a consistent change in the impedance signal could be followed with the increasing concentration of uPA (Figure 3). At low frequencies, the total impedance increased linearly within the 10 - 1000 pM uPA concentration range (Figure 3A, inset) and a similar tendency of the impedimetric signal variation was observed for the impedance phase shift (Figure 3B and S13, ESI). These results evidence higher sensitivity of the uPA analysis, with the K_d values of 0.15 nM and 0.02 nM estimated from the $|Z|$ - [uPA] and θ - [uPA] dependences, correspondingly (Table S1, ESI). Those values are at least one order of magnitude lower than the K_d obtained in the ferricyanide assay. The uPA-aptamer binding properties were also improved in presence of BSA, with the K_d for the formation of the aptamer–uPA–BSA complex of 0.001 nM (estimated from the phase shift), while in case of $|Z|$ there was no cleat tendency of signal change. The K_d values for the BSA binding to the aptamer-modified surface, calculated from the $|Z|$ and θ data, were of 6.66 nM and 0.09 nM, respectively (Figure S14, Table

S1, ESI). Thus, a non-specific interaction of BSA with the RNA-modified electrode surface appeared to be less pronounced at negative charges of the electrode surface, with MB as a redox indicator, than in the case of the ferricyanide assay.

On comparison of the data, a significant discrepancy in the K_d values estimated from such EIS parameters as $|Z|$ and θ can be followed, stemming from too small EIS signal variations. The overall reaction mechanism associated with MB interactions with the modified electrode seemed to be different from the diffusion-limited electrochemistry of ferricyanide, for which a well-defined charge-transfer semicircle was always observed. Presumably, different modes of interactions between MB and the RNA aptamer-modified electrode were responsible both for improved assay sensitivity and specificity and for insufficiently pronounced impedimetric signals. In the latter case, EIS was evidently not the best technique for analysis (Figure 3A), and cyclic voltammetry was used to improve the assay performance and study the reaction mechanism.

Voltammetric analysis of uPA with methylene blue as a redox indicator

CV analysis of the MB redox transformation at the RNA-aptamer-modified electrodes revealed a characteristic couple of redox peaks with a mean potential of -223±4 mV and a linear peak current variation with a square root of the potential scan rate (Figure 4). Thus, the overall ET reaction was limited by the MB diffusion to the electrode surface [64] with the ET rate constant of 0.019 cm s^{-1} estimated by the Nicholson approach[65] Therewith, the cathodic process was characterized rather by a wave than a peak, which complicated the analysis of "peak" current values.

Binding of uPA to the RNA-aptamer-modified electrode resulted in a change of a voltammetric wave form and a 13 mV positive shift in the mean peak potential value, to -210±4 mV (Figure 4B, Figure 5, inset), correlating with a higher positive charge in the EDL induced by binding of the positively charged uPA. After protein binding, the ET reaction became a surface-controlled process, characterised by the linear dependence of the MB peak currents on the potential scan rate. ET rate constant, k_{ET}, estimated by the Laviron approach[66] was 80.8 s^{-1}. Identical transitions from the diffusion-limited to surface-confined electrochemistry was also observed for uPA binding to the RNA-aptamer-modified surface in the presence of 100 nM BSA and for nonspecific adsorption of BSA, with the k_{ET} of 55.3 s^{-1} and 97.3 s^{-1}, correspondingly.

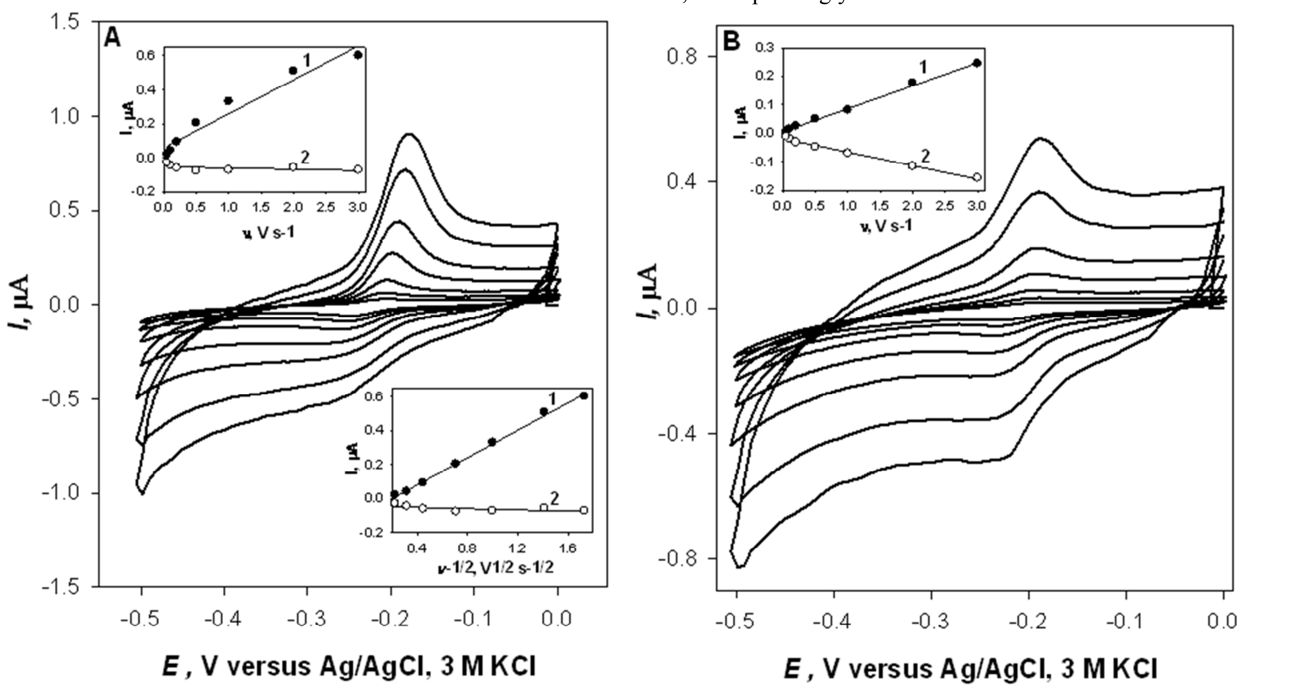

Fig. 4. Representative CVs for recorded with the RNA aptamer/MC_6OH-modified electrode in 1 µM MB solution in 20 mM PBS, pH 7.4, (A) before and (B) after incubation in 100 nM uPA; potential scan rate changes from 3 to 0.05 V s^{-1}. Insets: Dependence of the CV peak currents on the scan rate/square root of the scan rate.

Binding of the increasing amounts of uPA to the RNA aptamer tethered to the Au surface resulted in a gradual decrease in the MB signal, starting already from 1 pM uPA (Figure 4) and being particularly pronounced for anodic currents (I_{anodic}). Protein binding to the aptamer-modified electrode surface hindered free diffusion of MB to the electrode and resulted in the surface-confined ET reaction of MB molecules, then adsorbed on the protein. The balance of these two reactions resulted in the decreasing voltammetric signal with the increasing concentration of uPA. Interestingly, the extent of the signal decrease was different in CV and DPV (Figure 5), due to different abilities of these two techniques to discriminate between the surface-confined and diffusion limited ET reaction.[67, 68]

Thus, CV analysis enabled to correlate the minor EIS signal variations with the change in the mechanism of ET after protein binding to the aptamer-modified surface. Therewith, MB molecules are known to bind to any protein molecules[44]. The surface concentration of proteins can be different and, in our case, depended on the specificity and strength of the protein binding to the modified surface. The CV data were fitted to the Langmuir adsorption and Scatchard models (Eqs. 1 and 2) with S expressed as a relative current change $(I_0-I)/I_0$ ($I_0 = I_{anodic}^{max}$ recorded in 1 µM MB before the reaction with proteins).

A dramatic improvement of the aptamer binding properties could be followed at the negatively charged electrode surface: the K_b (reflecting the protein binding-dissociation equilibrium during formation of the uPA-aptamer complex) increased to 86.74, while the dissociation constant dropped down to 0.012 nM, by this three orders of magnitude improvement in the specificity and strength of binding being achieved. These data were consistent with the results of impedimetric measurements. The RNA aptamer affinity for uPA was further increased in the presence of BSA, reflected in the K_b and K_d of 367 and 0.003 nM, respectively (Figures 5, inset, and S15, ESI). Though nonspecific interactions of BSA with the aptamer-modified surface were not eliminated (Figures 5, inset, and S16, ESI), the false-positive signal induced by this process became less significant in the assay with MB (Table 1), with less than 30% signal interference from BSA once uPA was present in solution (uPA unsaturated conditions).

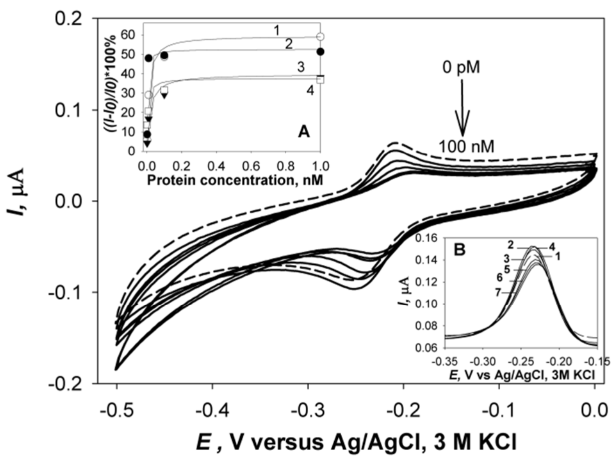

Fig. 5. Representative CVs recorded with the aptamer/MC_6OH-modified electrode in 1 µM MB solution in 20 mM PBS, pH 7.4, (dashed line) before and (solid lines) after incubation in uPA solutions of different concentrations, potential scan rate 0.1 V s^{-1}. Insets: (A) Dependence of the normalised I_{anodic} signal on the concentration of (1) uPA, (2) uPA and 100 nM BSA, (3) BSA and (4) uPA in 10% serum. Data were fitted to the Langmuir adsorption and Scatchard's models. (B) Representative DPVs recorded with the aptamer/MC_6OH-modified electrode in (1) 20 mM PBS and after incubation in (2) 1 pM, (3) 10 pM, (4) 100 pM, (5) 1 nM, (6) 10 nM and (7) 100 nM uPA. All other conditions are the same as in the main figure.

Thus, in the assay with MB at the negatively charged electrode surface the uPA binding properties of the RNA aptamer were improved compared to the assay with ferricyanide, at the positively charged electrode surface. This can be attributed to different modes of interactions between the redox indicators and the aptamer-modified electrodes. In one case, primarily the diffusion of ferricyanide to the electrode was affected by the free- and protein-bound aptamer-modified surface, while in another case, the principle reaction mechanism changed upon protein binding. In the absence of ligand the contribution of the upright (not lying flat) orientation of the negatively charged aptamer at the negatively charged electrode surface [67] may also contribute to the change in the ET mechanism responsible for the signal variation and better sensitivity of the assay. The aptamer freely standing at the negatively charged electrode surface may provide better surface access for diffusing MB molecules and be more accessible for protein binding as well. With protein binding the electrode surface becomes blocked and the overall process becomes limited by the ET reaction of MB bound to the protein-aptamer layer.

Electroanalysis of uPA in the presence of serum

Finally, the possibility of the uPA analysis in serum was assessed by both EIS with ferricyanide and CV analysis with MB as a redox indicator. In both cases, the intensity of measured signals essentially decreased for serum-containing samples, apparently due to nonspecific adsorption of serum proteins onto the aptamer-modified electrode surface (ESI, Figures S17 and S18, inset B). With ferricyanide as a redox indicator, fouling of the electrode surface by serum proteins was so strong, that that the variation of the EIS signal with the uPA concentration was insufficiently pronounced for the robust analysis of different concentration levels of uPA (Figure 2A, curve 4). Similar inhibitory effects of serum proteins on the aptasensor performance at positive charges of the electrode surface were observed in electroanalysis of theophylline[56]. Though the "alarm" signal from 1 nM uPA could be read out, its calibration was not feasible, which does not allow quantification of the uPA levels, important for cancer diagnosis. Neither the Langmuir isotherm nor to the Scatchard model gave reasonable fitting of the data.

In the assay with MB, despite the original decrease of the voltammetric signal intensity after the aptamer-modified electrode was exposed to the serum, a distinct calibration of the CV signal with the increasing uPA concentration in serum, starting from 1 pM uPA, was followed (Figure 5, inset A, and ESI, Figure S18). Data were fitted to the Scatchard model, yielding the dissociation constant K_d of 0.006 nM, this value being close to that observed for the uPA-aptamer binding in the presence of BSA (Table 1). Fitting of the data to the Langmuir isotherm was not possible, consistent with a higher complexity of the uPA adsorption behaviour in such complex biological medium as serum. The most important, in the case of the assay with MB as a redox indicator, performed at negative charges of the electrode surface, interference from serum proteins appeared to be not so detrimental as in the case of ferricyanide, and the robust quantification of the uPA content in serum can be done within the 1 pM – 1 nM concentration range clinically requested.

Conclusions

Here, electroanalysis of the cancer biomarker protein, uPA, was performed with a recently discovered uPA-specific RNA aptamer, tethered to gold electrode via enzymatically introduced phosphorothioated adenosine tag, and two indicators operating within different potential windows: ferricyanide and methylene blue, MB. Each of the redox indicators exhibited a distinct mode of interaction with the aptamer-modified surface. Protein assaying with ferricyanide was complicated by non-specific adsorption of BSA, though with a 1 nM detection limit and binding affinities consistent with the results reported for the solution biorecognition reaction. Electroanalysis with MB, at negative charges of the electrode surface, allowed sensitive and more specific 1 pM analysis of uPA, as a result of the improved apparent affinity of the surface-tethered RNA aptamer towards uPA. The advanced MB assay performance was associated with different mechanisms of MB-electrode interactions/proper orientation of the aptamer at the electrode surface and minimized interference from non-specific adsorption of BSA. Thus, electrochemical modulation of the aptamer state within the aptamer sensing layer was the key parameter in optimization of the aptamer - ligand interactions at the electrode surface. The results demonstrate the ability of the designed RNA aptamer sequence, integrated within the electrode format, to detect its ligand protein – cancer biomarker uPA – with a specificity and sensitivity sufficient for direct *in vivo* analysis.

Acknowledgements

This work has been supported by the Danish National Research Foundation through their support to the Centre for DNA Nanotechnology (CDNA-2), grant number DNRF81, and by the fellowship to M. Jarczewska provided by the European Union within the framework of the European Social Fund through the Warsaw University of Technology Development Programme realized by the Center for Advanced Studies.

Notes and references

[a] *Interdisciplinary Nanoscience Center (iNANO) and Center for DNA Nanotechnology (CDNA), Aarhus University, Gustav Wieds Vej 14, DK-8000 Aarhus C, Denmark. Tel: +45 8715 6703;*
E-mail: elena.ferapontova@inano.au.dk
[b] *Institute of Biotechnology, Department of Microbioanalytics, Faculty of Chemistry, Warsaw University of Technology, Noakowskiego 3, 00-664 Warsaw, Poland*
[c] *Department of Molecular Biology and Genetics, Aarhus University, Denmark*

† Electronic Supplementary Information (ESI) available: [details of any supplementary information available should be included here]. See DOI: 10.1039/b000000x/

1. R. Etzioni, N. Urban, S. Ramsey, M. McIntosh, S. Schwartz, B. Reid, J. Radich, G. Anderson and L. Hartwell, *Nature Reviews Cancer*, 2003, **3**, 243-252.
2. R. Bernards, *Cell*, 2010, **141**, 13-17.
3. V. Kulasingam and E. P. Diamandis, *Nature Clinical Practice Oncology*, 2008, **5**, 588-599.
4. J. A. Ludwig and J. N. Weinstein, *Nature Reviews Cancer*, 2005, **5**, 845-856.
5. C. L. Sawyers, *Nature*, 2008, **452**, 548-552.
6. T. A. Stamey, N. Yang and A. R. Hay, *New England Journal of Medicine*, 1987, **317**, 909-916.
7. H. Lilja, D. Ulmert and A. J. Vickers, *Nature Reviews Cancer*, 2008, **8**, 268-278.
8. D. J. Slamon, W. Godolphin, L. A. Jones, J. A. Holt, S. G. Wong, D. E. Keith, W. J. Levin, S. G. Stuart, J. Udove, A. Ullrich and M. F. Press, *Science*, 1989, **244**, 707-712.
9. R. Molina, J. M. Augé, J. M. Escudero, X. Filella, G. Zanon, J. Pahisa, B. Farrus, M. Muñoz and M. Velasco, *Tumor Biology*, 2010, **31**, 171-180.
10. I. J. Jacobs and U. Menon, *Molecular and Cellular Proteomics*, 2004, **3**, 355-366.
11. M. Felder, A. Kapur, J. Gonzalez-Bosquet, S. Horibata, J. Heintz, R. Albrecht, L. Fass, J. Kaur, K. Hu, H. Shojaei, R. Whelan and M. Patankar, *Molecular Cancer*, 2014, **13**, 129.
12. H. Stein, H. D. Foss, H. Durkop, T. Marafioti, G. Delsol, K. Pulford, S. Pileri and B. Falini, *Blood*, 2000, **96**, 3681-3695.
13. H. Iwagaki, A. Hizuta, H. Kohka, K. Kobashi, Y. Nitta, H. Isozaki, N. Takakura and N. Tanaka, *Journal of Medicine*, 1999, **30**, 111-121.
14. P. A. Andreasen, R. Egelund and H. H. Petersen, *Cellular and Molecular Life Sciences*, 2000, **57**, 25-40.
15. K. Danø, N. Behrendt, G. Høyer-Hansen, M. Johnsen, L. R. Lund, M. Ploug and J. Rømer, *Thrombosis and Haemostasis*, 2005, **93**, 676-681.
16. F. Blasi, J. D. Vassalli and K. Dano, *Journal of Cell Biology*, 1987, **104**, 801-804.
17. K. Dass, A. Ahmad, A. S. Azmi, S. H. Sarkar and F. H. Sarkar, *Cancer Treatment Reviews*, 2008, **34**, 122-136.
18. H. Biliran, Jr. and S. Sheng, *Cancer Res*, 2001, **61**, 8676-8682.
19. R. Drapkin, A. Clauss and S. Skates, *Clinical Cancer Research*, 2008, **14**, 5643-5645.
20. B. Hundsdorfer, H. F. Zeilhofer, K. P. Bock, P. Dettmar, M. Schmitt, A. Kolk, C. Pautke and H. H. Horch, *Journal of Cranio-Maxillofacial Surgery*, 2005, **33**, 191-196.
21. N. Harbeck, R. E. Kates, M. Schmitt, K. Gauger, M. Kiechle, F. Jänicke, C. Thomssen, M. P. Look and J. A. Foekens, *Clinical Breast Cancer*, 2004, **5**, 348-352.
22. D. S. Lang, U. Heilenkötter, W. Schumm, O. Behrens, R. Simon, E. Vollmer and T. Goldmann, *Breast*, 2013, **22**, 736-743.
23. C. B. Fowler, Y. G. Man and J. T. Mason, *Journal of Cancer*, 2014, **5**, 115-124.
24. A. N. Pedersen, H. T. Mouridsen, D. Y. Tenney and N. Brünner, *European Journal of Cancer*, 2003, **39**, 899-908.
25. E. J. Cho, J. W. Lee and A. D. Ellington, *Annu Rev Anal Chem*, 2009, **2**, 241-264.
26. A. B. Iliuk, L. Hu and W. A. Tao, *Anal. Chem.*, 2011, **83**, 4440-4452.
27. I. Willner and M. Zayats, *Angew. Chem. Int. Ed.*, 2007, **46**, 6408-6418.
28. T. Hianik and J. Wang, *Electroanalysis*, 2009, **21**, 1223-1235.
29. E. E. Ferapontova and K. V. Gothelf, *Current Organic Chemistry*, 2011, **15**, 498-505.
30. J. Liu, M. D. a. Morris, F. C. Macazo, L. R. Schoukroun-Barnes and R. J. White, *J. Electrochem. Soc.*, 2014, **161** H301-H313.
31. A. D. Ellington and J. W. Szostak, *Nature Struct. Biol.*, 1990, **346**, 818-822.
32. R. C. Conrad, L. Giver, Y. Tian and A. D. Ellington, *Method Enzymol.*, 1996, **267**, 336-367.
33. T. Hermann and D. J. Patel, *Science*, 2000, **287**, 820-825.
34. M. Lutzelberger, M. R. Jakobsen and J. Kjems, in *Handbook of RNA Biochemistry*, ed. R. K. Hartmann, Wiley-VCH Verlag GmbH & Co. KGaA, Weinheim, Germany 2005, vol. 2, pp. 878-894.
35. B. R. Baker, R. Y. Lai, M. S. Wood, E. H. Doctor, A. J. Heeger and K. W. Plaxco, *J. Am. Chem. Soc.*, 2006, **128**, 3138-3139.
36. X. Zuo, S. Song, J. Zhang, D. Pan, L. Wang and C. Fan, *J. Am. Chem. Soc.*, 2007, **129**, 1042-1043.
37. X. Zuo, Y. Xiao and K. W. Plaxco, *J. Am. Chem. Soc.*, 2009, **131**, 6944-6945.
38. E. E. Ferapontova and K. V. Gothelf, *Electroanalysis*, 2009, **21**, 1261-1266.
39. E. Farjami, R. Campos, J. Nielsen, K. Gothelf, J. Kjems and E. E. Ferapontova, *Anal. Chem.* , 2013, **85**, 121-128.
40. L. Shen, Z. Chen, Y. Li, P. Jing, S. Xie, S. He, P. He and Y. Shao, *Chem.Commun.*, 2007, 2169-2171.
41. Y. Xiao, B. D. Piorek, K. W. Plaxco and A. J. Heeger, *J. Am. Chem. Soc.*, 2005, **127**, 17990-17991.
42. H.-M. So, K. Won, Y. H. Kim, B.-K. Kim, B. H. Ryu, P. S. Na, H. Kim and J.-O. Lee, *J. Am. Chem. Soc.*, 2005, **127**, 11906-11907.
43. F. Le Floch, H. A. Ho and M. Leclerc, *Anal. Chem.*, 2006, **78**, 4727-4731.
44. T. Hianik, V. Ostatná, M. Sonlajtnerova and I. Grman, *Bioelectrochemistry*, 2007, **70**, 127-133.
45. M. C. Rodriguez, A.-N. Kawde and J. Wang, *Chem.Commun.*, 2005, 4267-4269.
46. R. Y. Lai, K. W. Plaxco and A. J. Heeger, *Anal. Chem.*, 2007, **79**, 229-233.
47. Y. L. Zhang, Y. Huang, J. H. Jiang, G. L. Shen and R. Q. Yu, *J. Am. Chem. Soc.*, 2007, **129**, 15448-15449.

48. Y. Liu, N. Tuleouva, E. Ramanculov and A. Revzin, *Anal Chem*, 2010, **82**, 8131-8136.
49. D. M. Dupont, J. B. Madsen, R. K. Hartmann, B. Tavitian, F. Ducongé, J. Kjems and P. A. Andreasen, *RNA*, 2010, **16**, 2360-2369.
50. E. E. Ferapontova, *Current Analytical Chemistry*, 2011, **7**, 51-62.
51. T. Hianik, V. Ostatná, Z. Zajacová, E. Stoikova and G. Evtugyn, *Bioorg. Med. Chem. Lett.*, 2005, **15**, 291-295.
52. A. K. H. Cheng, B. Ge and H.-Z. Yu, *Anal. Chem.*, 2007, **79**, 5158-5164.
53. R. Campos, A. Kotlyar and E. E. Ferapontova, *Langmuir*, 2014, **30** 11853–11857.
54. E. E. Ferapontova, E. M. Olsen and K. V. Gothelf, *J. Am. Chem. Soc.* , 2008, **130**, 4256-4258.
55. H. A. Krebs, *Ann. Rev. Biochem.*, 1950, **19**, 409-430.
56. E. E. Ferapontova and K. V. Gothelf, *Langmuir*, 2009, **25**, 4279-4283.
57. X. Luo, Q. Xu, T. James and J. J. Davis, *Anal. Chem.*, 2014, **86**.
58. M. Silvestrini, P. Schiavuta, P. Scopece, G. Pecchielan, L. M. Moretto and P. Ugo, *Electrochim. Acta*, 2011, **56**, 7718-7724.
59. B. Hoyer and N. Jensen, *Electroanalysis*, 2005, **17**, 2037-2042.
60. A. J. Bonham, N. G. Paden, F. Ricci and K. W. Plaxco, *Analyst*, 2013, **138**, 5580-5583.
61. A. Bogomolova, E. Komarova, K. Reber, T. Gerasimov, O. Yavuz, S. Bhatt and M. Aldissi, *Anal. Chem.*, 2009, **81**, 3944-3949.
62. A.-E. Radi, J. L. A. Sánchez, E. Baldrich and C. K. O'Sullivan, *Anal. Chem.*, 2005, **77**, 6320-6323.
63. M. J. Greig, H. Gaus, L. L. Cummins, H. Sasmor and R. H. Griffey, *J. Am. Chem. Soc.*, 1995, **117**, 10765-10766.
64. A. J. Bard and L. R. Faulkner, *Electrochemical Methods - Fundamental and Applications*, Wiley, New York, 1980.
65. R. S. Nicholson, *Anal. Chem.*, 1965, **37**, 1351-1355.
66. E. Laviron, *J. Electroan. Chem.*, 1979, **101**, 19-28.
67. E. Farjami, R. Campos and E. E. Ferapontova, *Langmuir*, 2012, **28**, 16218-16226.
68. E. Farjami, L. Clima, K. Gothelf and E. E. Ferapontova, *Anal. Chem.*, 2011, **83**, 1594-1602.